Article

A Basic Study on Hybrid Systems for Small Race Car to Improve Dynamic Performance Using Lap Time Simulation

Ikkei Kobayashi [1], Kazuki Ogawa [2], Daigo Uchino [2], Keigo Ikeda [3], Taro Kato [4], Ayato Endo [5], Mohamad Heerwan Bin Peeie [6], Takayoshi Narita [7,*] and Hideaki Kato [7]

1   Course of Mechanical Engineering, Tokai University, Kitakaname 4-4-1, Hiratsuka 259-1292, Japan; 2cemm030@mail.u-tokai.ac.jp
2   Course of Science and Technology, Tokai University, Kitakaname 4-4-1, Hiratsuka 259-1292, Japan; 0ctad005@mail.u-tokai.ac.jp (K.O.); 1ctad002@mail.u-tokai.ac.jp (D.U.)
3   Department of Mechanical Engineering, Hokkaido University of Science, 7-Jo 15-4-1 Maeda, Sapporo 006-8585, Japan; ikeda-k@hus.ac.jp
4   Department of Mechanical Engineering, Tokyo University of Technology,1404-1 Katakuramachi, Hachioji 192-0982, Japan; katohtr@stf.teu.ac.jp
5   Department of Electrical Engineering, Fukuoka Institute of Technology, 3-30-1 Wajiro-higashi, Fukuoka 811-0295, Japan; endo@fit.ac.jp
6   Faculty of Mechanical and Automotive Engineering Technology, University Malaysia Pahang, Paken 26600, Malaysia; mheerwan@ump.edu.my
7   Department of Mechanical Systems Engineering, Tokai University, Kitakaname 4-4-1, Hiratsuka 259-1292, Japan; hkato@tokai-u.jp
*   Correspondence: narita@tsc.u-tokai.ac.jp; Tel.: +81-463-58-1211

Abstract: A hybrid vehicle is a vehicle with two or more power sources. We propose a hybrid system in which the engine torque converted by the transmission is combined with an electric motor torque. The proposed system reduces transmission because engine torque only acts during transmission. Furthermore, the proposed hybrid system's simple structure uses lightweight chains and sprockets that can be laid out in various ways. The realization of the proposed hybrid system requires independent control algorithms for the two power systems, engine and electric motor, that take into consideration the state of the vehicle and the driver's input; this system can be assumed to be a servo model system with multiple inputs and outputs and analyzed to obtain the optimal operation algorithm. To apply these controls to race cars, which are required to be fast, it is necessary to obtain the reference input, which is the optimal velocity and yaw angle while traveling the course of the servo system, and simulations of the competition track must be carried out. Therefore, the dynamic performance of the hybrid system was investigated by calculating the lap times on a given circuit using a quasi-steady-state method with low computational load and high prediction accuracy. In this study, the effects of changing the electric motor and final gear ratios on the driving performance of a rear-wheel-drive parallel hybrid system for optimization were investigated. The simulation results show that not only can the optimum settings be obtained by changing the final and electric motor reduction ratios on the evaluation circuit, but also that the optimum values vary across different speed ranges on different circuits.

Keywords: hybrid system; small vehicle; dynamic performance; lap time simulation

1. Introduction

A hybrid vehicle is a vehicle with multiple forms of motive power. Recently, hybrid vehicles, which are powered by two systems, an internal combustion engine (ICE) that generates high power at high rotational speeds, and one or more electric motors that generate high power at low rotational speeds, have been marketed by many vehicle manufacturers for their energy efficiency; these vehicles use the electric motor to compensate for the lack of low-speed torque in gasoline-powered vehicles, and high torque and acceleration

can be expected in the lower speed range. Because of these advantages, general vehicles with hybrid systems that have been put on the market in recent years aim to reduce fuel consumption by downsizing the ICE. There has been much research on hybrid systems for energy management and comfortable driving, with the main focus on improving fuel economy [1–5]; however, these studies were also conducted on hybrid powertrains such as conventional series, parallel, power split, and series-parallel [6]. These systems combine the power of the ICE and electric motor using gears or planetary gears [7] but have drawbacks, such as heavy system weight and limited component layout. In addition, some automobile companies began to sell vehicles for one or two passengers as personal mobility, used for short-distance transfers. Although the vehicles are expected to be installed for personal mobility, it is difficult to install a conventional hybrid system owing to its compactness. Furthermore, in most of the previous hybrid systems, the electric motor torque is combined with the ICE torque before a reduction mechanism, e.g., transmission or torque converter. In other words, the electrical motor in conventional vehicles assists the ICE depending on the rotational speed; however, most required cases of electric motor torque is the low velocity of the vehicle, owing to the torque characteristics of the ICE at low rotational speeds. Therefore, we propose a hybrid system in which the ICE torque converted by the transmission is combined with electric motor torque. The proposed system can reduce transmission because the ICE torque only acts on the transmission. Furthermore, the proposed hybrid system has a simple structure using lightweight chains and sprockets that can be laid out in various ways [8]. Figure 1 shows the circuit schematic of the conventional and hybrid system proposed in this report.
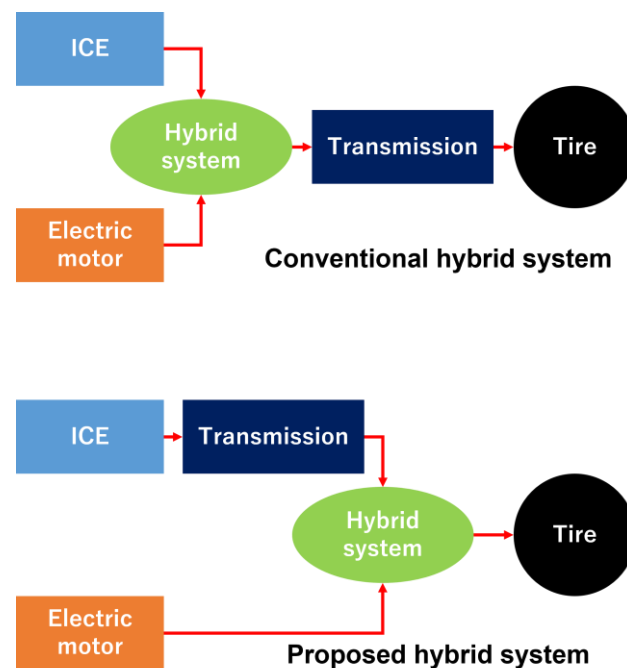

Figure 1. Schematic of the conventional and proposed hybrid systems.

In addition, because hybrid vehicles are equipped with multiple power sources with different characteristics, the characteristics of the hybrid powertrain will strongly depend on the operating algorithm running on the powertrain's control unit. If the hybrid system is operated optimally, not only fuel efficiency characteristics, but also dynamic performance can be improved. In recent years, hybrid systems powered by ICEs and electric motors have begun to be used in race cars, where high vehicle powertrain performance is requested. In race cars, the main concern is to improve the vehicle performance of the powertrain, which consists of an ICE and an electric motor, and to minimize lap times, as it is the most important objective of winning the competition. To be fast on a given circuit, the

acceleration performance needs to be improved, particularly to reach maximum speed in a short time. Other concepts include In-Wheel-Motor-Driven Electric Vehicles with electric motors mounted on each wheel; these have the advantage of being able to use all tires for driving forces and of implementing independent control of all four wheels, but they also have problems in terms of the vehicle dynamic performance of the competition vehicle, such as increased unsprung mass and moment of inertia. Since the proposed system is laid out with heavy elements such as the ICE and the electric motor near the center of gravity on the chassis, we consider it to be well-placed to solve the above problems and achieve higher performance. In previous studies, the optimal battery control method for hybrid systems to minimize lap times and a comparison of acceleration performance between two different power system layouts have been reported [9,10], but not enough has been done to investigate the more active use of hybrid systems for driving performance; particularly, the consideration of a hybrid system for small cars has not been reported. Therefore, we focused on Formula Hybrid, which is a competition for small hybrid racing cars, and developed a hybrid drive system for those vehicles.

The realization of the proposed hybrid system requires independent control of the two power systems, ICE and electric motor, taking into consideration the vehicle status, and driver input; this system can be assumed to be a servo model system [11,12] with multiple inputs and outputs and analyzed to obtain the optimal operation algorithm. To apply these controls to race cars, which are required to be fast, it is necessary to obtain the reference input, which is the optimal velocity and yaw angle while traveling the course of the servo system, and simulations of the competition track must be carried out.

In addition, it is necessary to predict the speeds that can be achieved by the vehicle on a predetermined circuit, and simulations of the competition track must be performed.

A lap-time simulation was used to predict the performance of the vehicle within a given circuit. The simulation is primarily a tool to predict the effect of various vehicle elements on lap time, and can also track vehicle maneuvering. There are many types of simulation methods, ranging from simple steady-state simulations to multi-body simulations involving complex transient phenomena [13–16].

Previous studies have reported the usefulness of quasi-steady-state simulations in terms of computational load and time-prediction accuracy [17,18]. Non-linear tire [19] and four-wheel models [20] considering load transfer have also been applied to tire characteristics; however, these studies were conducted on vehicles powered only by ICEs, and the effect of the hybrid system's output characteristics proposed by the authors on decreasing lap time on a circuit consisting of several straight lines and corners with different curvatures was not sufficiently investigated.

Therefore, the dynamic performance of the hybrid system was investigated by calculating the lap times on a given circuit using a quasi-steady-state method with low computational load and high prediction accuracy. In this study, the effects of changing the electric motor and final gear ratios on the driving performance of a rear-wheel-drive parallel hybrid system for optimization were investigated. Since the study is concerned only with the impact of dynamic performance, a simple vehicle model was used in the lap time simulation, in which load transfer, differential mechanism, and nonlinear tire characteristics were not considered.

2. Small Racing Car Installed Proposed Hybrid System

2.1. Outline of Proposed Hybrid Racing Car

Figure 2 shows an outline of a small hybrid racing car for improving the dynamic performance of vehicles. The coordinates were set as shown in this figure. Accelerations x and y in the longitudinal and lateral directions, respectively, and angular acceleration ψ in the vertical direction were detected by an acceleration sensor installed near the vehicle's center of gravity. The longitudinal velocity x of the vehicle was detected using a speed sensor installed at the output shaft. The detected accelerations and velocity are sent to a digital signal processor (DSP) via an analog-to-digital (A/D) converter. The controller

installed in the DSP feeds back these values and other output-control signals to an engine control unit (ECU) and an electric motor driver via a digital-to-analog(D/A) converter. The ECU and electric motor driver operate the ICE and electric motor, respectively, to generate torque from the ICE T_e and torque from the electric motor T_m; these generated torques are amplified by a reduction mechanism using chains and sprockets, and are then transferred to a proposed hybrid mechanism. The combined torque is transmitted to the tires as traction force via the final reduction gear.
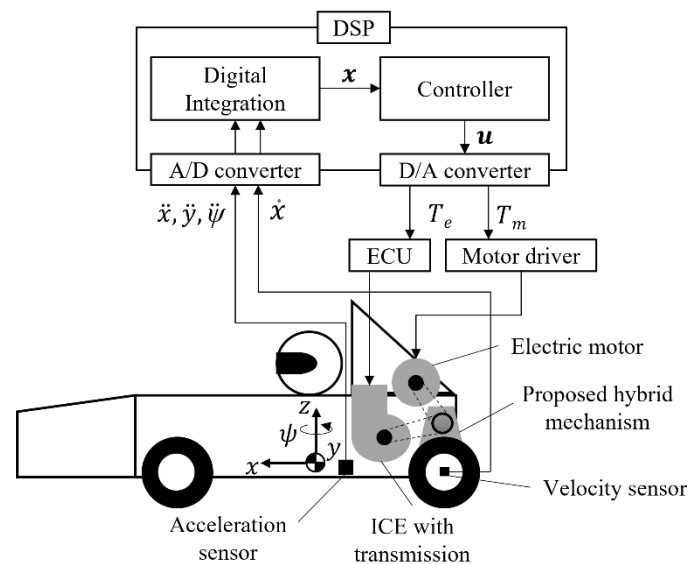

**Figure 2.** Outline of proposed hybrid racing car.

In addition, there is a trade-off relationship where comfort decreases as dynamic performance is pursued; however, the method proposed in this paper will not be a problem when applied to race cars, where the emphasis is on dynamic performance. On the other hand, when the present system is applied to passenger car, comfort is likely to be an important factor. In this case, it is considered that one solution to ensure comfort without sacrificing dynamic performance would be to apply active control that dampens the driver himself. For example, a solution would be to build and implement a system that can control lateral translational motion and rotational motion of roll, pitch, and yaw, in addition to vertical control as currently installed in truck seats.

2.2. Structure of the Hybrid System

In general, the torque of the ICE is low at low rotational speeds and increases with an increase in the rotational speed before the torque peak. In contrast, the torque of the electric motor is high at low rotational speeds and decreases with increasing rotational speed. In recent hybrid vehicles, the electric motor torque is combined with the ICE torque before a reduction mechanism, e.g., a transmission or torque converter. In other words, the electric motor in conventional vehicles assists the ICE, depending on the rotational speed. Therefore, we propose a hybrid system in which the ICE torque converted by the transmission is combined with electric motor torque. The proposed system can reduce transmission because the ICE torque only acts on the transmission.

The proposed hybrid system is equipped with a proposed hybrid mechanism instead of the planetary gear transmission system used in many passenger cars. Planetary gears have many layout restrictions and are difficult to maintain, whereas the proposed hybrid mechanism has the advantages of easy maintenance, fewer design requirements on the chassis side, and the ability to use a chain, making it easy to lay out. In this study, we installed a motorcycle ICE integrated with a transmission in the proposed hybrid system. Figure 3a shows a 3D model of the proposed hybrid system; this system comprises an ICE,
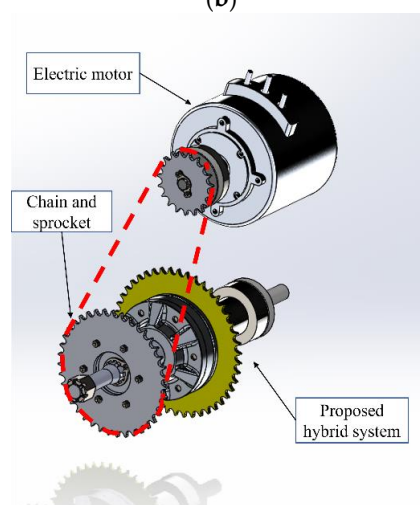
electric motor, and a proposed hybrid mechanism, and these elements are connected by sprockets and a chain, as shown in Figure 3b,c.
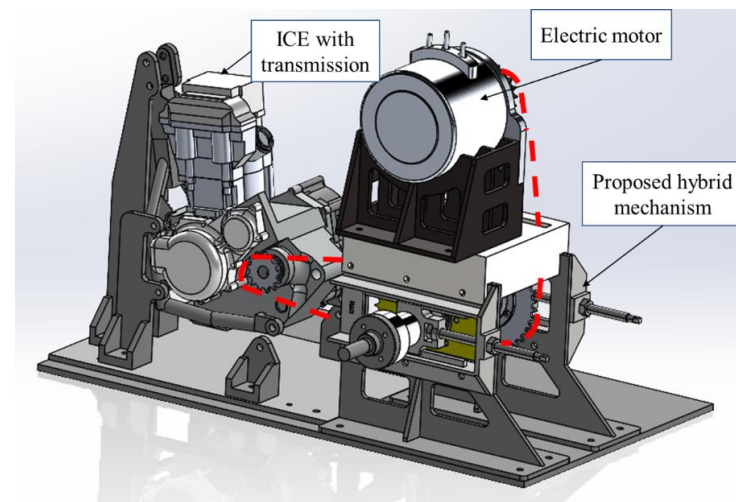
(**a**)
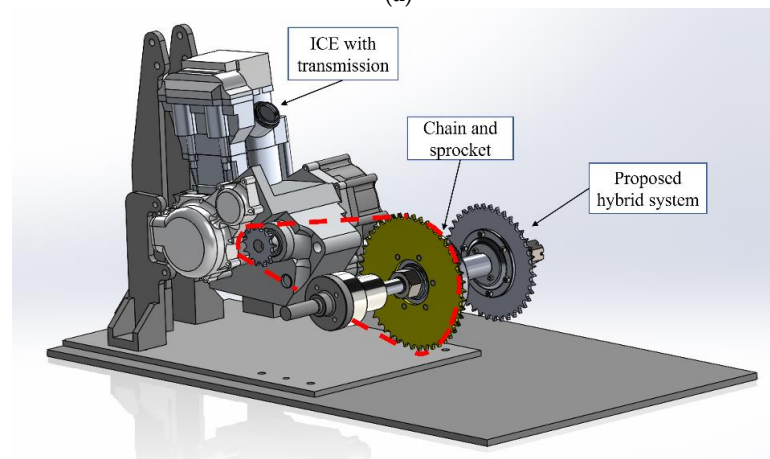
(**b**)

(**c**)

Figure 3. 3D model of the hybrid system. (**a**) Brids view. (**b**) Connection between the ICE and proposed hybrid mechanism. (**c**) The connection between the electric motor and the proposed hybrid mechanism.

Figure 4 shows a schematic diagram of the proposed hybrid system. As shown in Figure 4a, during acceleration in the proposed hybrid system, the shaft torque generated by the ICE is shifted via the transmission, decelerated, transmitted from the ICE sprocket to the drive shaft side sprocket by a chain, and then to the axle shaft via the one-way clutch and final gear. The shaft torque generated by the electric motor is decelerated and transmitted to the drive shaft side sprocket by a chain, and then transmitted to the axle by the final gear. The drive torque generated around the tire is the sum of the above two torques transmitted to the axle shafts.
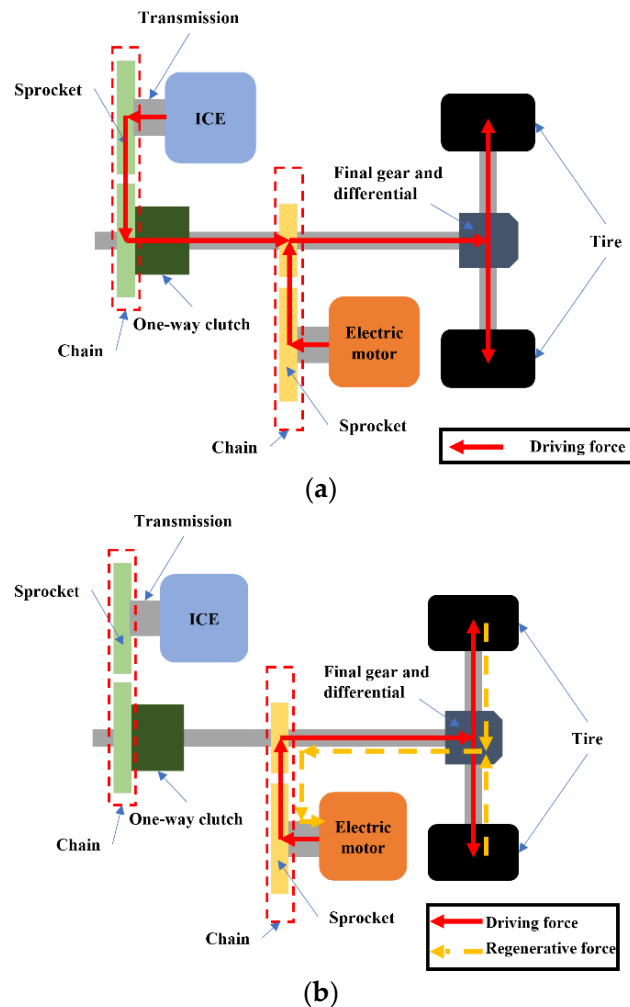

Figure 4. Proposal of a device for combining traction force generated by an ICE and electric motor. (**a**) Acceleration. (**b**) Deceleration.

Conversely, during deceleration, as shown in Figure 4b, there is no drive power from the ICE, the electric motor drive power is not transmitted to the ICE via the one-way clutch, and the ICE sprocket on the drive shaft side idles. In addition, the braking force on the tire contact patch generates torque on the axle shaft in the opposite direction of acceleration, which is transmitted to the electric motor shaft by the final gear and sprockets; these torques generate power in the electric motor and regenerate energy.

2.3. Two Power Sources in a Hybrid System

The ICE in the hybrid system was the G363E used in the YAMAHA WR250R, and shown in Figure 5. Table 1 lists the specifications of the ICE, and Figure 6 shows the two-dimensional data of the relationship between the rotational speed and torque.

Figure 5. ICE of G363E manufactured by Yamaha Motor Co., Ltd., Iwata, Japan.

Table 1. Specifications of the ICE.

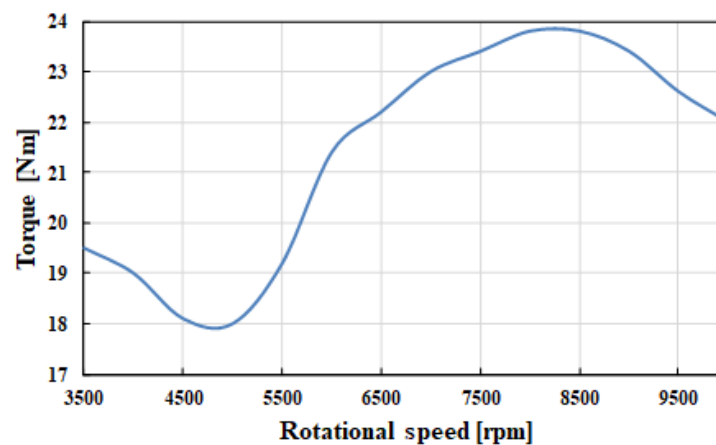| Engine Model Number	G363E
Engine Type	250 cc liquid-cooled DOHC 4-stroke, 4 valves
Bore × Stroke	77.0 mm × 53.6 mm
Compression Ratio	11.8:1
Fuel Delivery	Fuel injection
Ignition	TCI: Transistor Controlled Ignition
Transmission	Constant mesh 6-speed, multiplate wet clutch
Max Power	23 kW/10,000 rpm
Max Torque	24 Nm/8000 rpm

Figure 6. Relationship between ICE rotational speed and torque.

The electric motor in the hybrid system is specified to have a maximum output of less than 30 kW and uses an air-cooled Motenergy ME0913 brushless motor, as shown in Figure 7. Table 2 lists the specifications of the electric motor, and Figure 8 shows the relationship between the rotational speed and torque.

Figure 7. Electric motor Motenergy ME0913.

Table 2. Specifications of the electric motor.

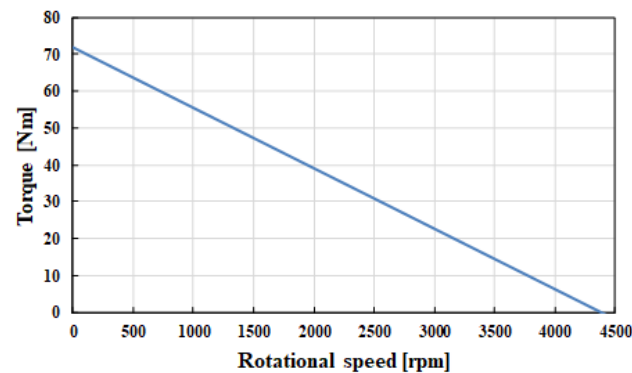|	
Drive voltage	DC 24 V–96 V
Maximum current	550 A
Maximum rotation speed	5000 rpm (No load)
Maximum output	30 kW (DC 96 V)
Maximum torque	90 Nm
Continuous output	12 kW (DC 96 V)
Continuous current	180 A
Continuous efficiency	92 %
Continuous rotation speed	3000 rpm
Mass	15.9 kg
Poles	4 (Magnet 8)
Cooling method	Air cooling forced fan system

Figure 8. Relationship between motor rotational speed and torque.

2.4. Control Model of the Hybrid System

In Section 2.1, the dynamic states of the hybrid vehicle in longitudinal, lateral, and vertical rotational directions were described; these state variables are expressed as state vector x in Equation (1).

$$x = \left\{ x\ \dot{x}\ y\ \dot{y}\ \psi\ \dot{\psi} \right\}^{\mathrm{T}} \tag{1}$$

The drivers or systems operate the ICE, electric motor, brake, and steering wheel; these factors are assumed as control inputs for the hybrid vehicle and expressed as the control input vector u in Equation (2).

$$u = \{T_{\mathrm{e}}\ T_{\mathrm{m}}\ F_{\mathrm{b}}\ \delta_{\mathrm{f}}\}^{\mathrm{T}} \tag{2}$$

Therefore, the vehicle that includes the proposed hybrid system can be assumed to be a multiple-input and multiple-output system, expressed in the state equation as follows:

$$\dot{x} = Ax + Bu \tag{3}$$

where the system matrix A and control matrix B are the dynamic characteristics of the proposed hybrid vehicle. Furthermore, the output equation of the vehicle is expressed as Equation (4). Note that, since the purpose of this report is to examine the advantages of the proposed hybrid system, system uncertainties and disturbances are not considered. In the future, since they are necessary for implementation. Robust control theories, such as sliding mode and μ-synthesis, will be introduced to improve the system.

$$y = Cx \tag{4}$$

y is the system output and C is the output matrix.

The vehicle travels at a speed $\dot{x}$ and vertical angle ψ in local coordinates fixed to the vehicle relative to the global coordinates, as shown in Figure 9. The dashed line indicates the operation trajectory. If the vehicle traces this trajectory at the optimal velocity obtained from vehicle dynamics, the vehicle can travel the course in the fastest time; an extremely important factor in demonstrating the dynamic performance of the vehicle. The optimum vehicle velocity $\dot{x}_{des}$, lateral displacement y_{des}, and yaw angle of the vehicle ψ_{des} were set along the trajectory; these values are assumed to be reference inputs in a servomechanism, and are expressed as a reference input vector in Equation (5).

$$\boldsymbol{r} = \left\{ \dot{x}_{des} \ y_{des} \ \psi_{des} \right\}^{\mathrm{T}} \tag{5}$$

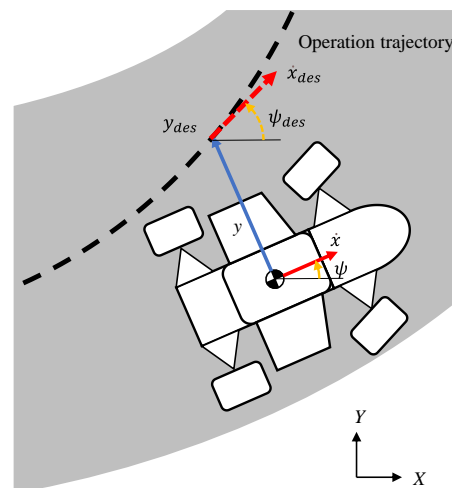**Figure 9.** Coordinates of the vehicle and reference trajectory.

The control error e is the difference between the system output $\boldsymbol{y}$ and the reference input $\boldsymbol{r}$ are as follows:

$$e = r - y = r - Cx \tag{6}$$

The state variable vector $\boldsymbol{z}$ is defined as the time integration of the variable vector $\boldsymbol{e}$.

$$\dot{z} = e \tag{7}$$

Combining these equations, the expanded system can be expressed as follows:

$$\begin{pmatrix} \dot{x} \\ \dot{z} \end{pmatrix} = \begin{pmatrix} A & 0 \\ -C & 0 \end{pmatrix} \begin{pmatrix} x \\ z \end{pmatrix} + \begin{pmatrix} B \\ 0 \end{pmatrix} u + \begin{pmatrix} 0 \\ r \end{pmatrix} \tag{8}$$

It is expected that an optimal control algorithm to drive faster can be obtained using this equation; however, it is necessary to obtain the optimal reference input $\boldsymbol{r}$ such as the trajectory in Figure 9. In this study, we aimed to obtain the optimal velocity of the reference input by initially focusing on the motion in the longitudinal direction.

3. Calculation Method Using Quasi-Steady-State Lap Time Simulation

In this simulation, the vehicle was assumed to always be in equilibrium, and the yaw motion was ignored. The velocity in each section is determined as the maximum velocity attainable when driving within the range of a three-dimensional map consisting of lateral acceleration, longitudinal acceleration, and speed; this is called the GGV vehicle performance envelope, and is pre-calculated from the vehicle model. Figure 10 shows a schematic of the GGV vehicle performance envelope. The performance of longitudinal and lateral accelerations is seen to increase or decrease depending on the magnitude of the velocity. Generally, changes in velocity affect the vehicle's friction ellipse owing to aerodynamics and ICE speed.
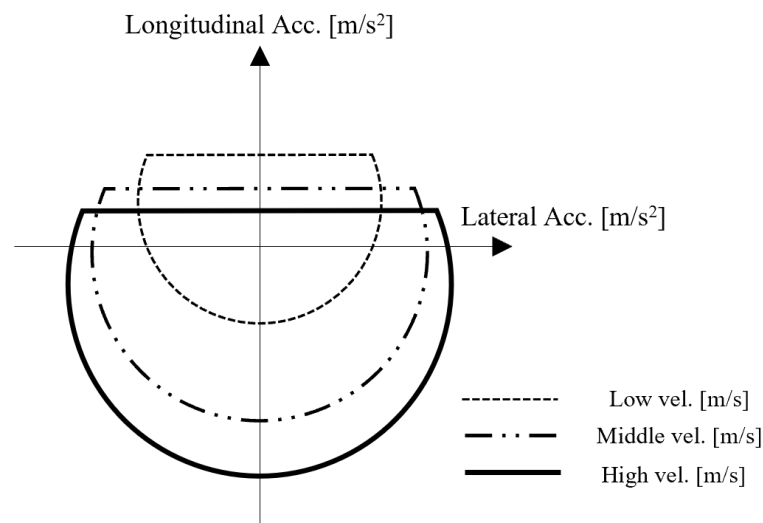

Figure 10. Schematic of the GGV vehicle performance envelope.

The lap time is calculated by discretizing and summing the times for each and all segments, respectively.

3.1. Simplified Vehicle Model

To simplify the calculations, the forces acting on the four tires of the vehicle are assumed to be those at the center of gravity, as shown in Figure 11; this simple assumption neglects the load transfer in the longitudinal and lateral directions. The lateral and longitudinal forces $F_{x,y}$ at the tire contact patch were calculated from the simplified linear tire model shown in (9) by multiplying the vertical load F_z by the friction coefficients in the lateral and longitudinal directions $\mu_{x,y}$.
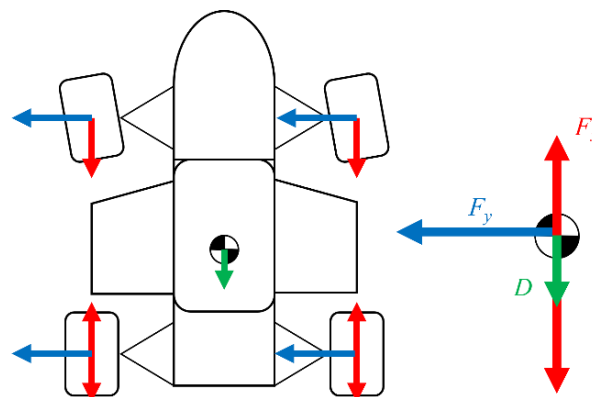

Figure 11. Vehicle model with simple assumptions.

The vertical load is the weight produced by the vehicle mass m, acceleration of gravity g, and aerodynamic function downforce L, which is calculated using Equation (10). The downforce is then calculated in Equation (11) and is found to be a function of the speed v.

$$F_{x,y} = F_z \cdot \mu_{x,y} \tag{9}$$

$$F_z = mg + L \tag{10}$$

$$L = 0.5 \cdot C_L A \rho v^2 \tag{11}$$

The tractive force F_t derived from the hybrid powertrain system is calculated from the vehicle speed v, each gear ratio gr, and tire radius r_t, using Equation (12) to calculate the ICE speed, electric motor speed ω. The shaft torque T of the two systems from these rotational speeds are combined and calculated in Equation (13) using the tire radius.

$$\omega = \frac{v \cdot gr}{r_t} \tag{12}$$

$$F_t = \frac{v \cdot gr}{r_t} \tag{13}$$

The lower of the tire longitudinal and powertrain-derived driving forces obtained in Equations (9) and (13), respectively, are used as the longitudinal force at the vehicle's center of gravity; this is because the longitudinal force at the tire contact patch is highly dependent on the slip ratio, which is the ratio of the vehicle's speed to the tire's rotational speed, generated by the drive torque and varies only slightly; therefore, the approximation in Equation (14) is used. Longitudinal forces at the vehicle's center of gravity can be calculated by taking into consideration the drag force D of the aerodynamic function. The drag force is a function of speed, as is the downforce in Equation (11), and can be calculated in Equation (15) using the drag coefficient C_D.

$$T \approx F_x \cdot r_t \tag{14}$$

$$D = 0.5 \cdot C_D A \rho v^2 \tag{15}$$

Using the above calculations, it is possible to calculate the maximum lateral and longitudinal forces for each velocity. To calculate the combined state in which these longitudinal and lateral forces occur simultaneously in the quasi-steady state, the friction ellipse assumption in Equation (16) is used.

$$\left(\mu_{x,y} \cdot F_z \right)^2 = F_x^2 + F_y^2 \tag{16}$$

3.2. Calculation Method for Lap Time in Quasi-Steady State

The quasi-steady-state lap time simulation in this research was calculated from pre-discretized circuit data of the radius of curvature and distance; these can be obtained using GPS and data-logging systems installed in actual vehicles.

First, a critical speed profile is created in Equation (17) using the corner radius R and maximum lateral acceleration ay calculated from the vehicle model. At this time, the velocity within each section is not within the GGV vehicle performance envelope when longitudinal acceleration occurs, owing to the maximum lateral acceleration. To solve this problem, the critical speed profile is used to calculate the longitudinal acceleration a_x of velocity v within the adjacent section distance dx from the beginning to the end of the circuit using Equation (18), and the acceleration and deceleration velocities are calculated by decreasing the velocity until it falls within the GGV vehicle performance envelope. An

illustration showing the calculation of acceleration and deceleration side velocities within an adjacent section is presented in Figure 12.

$$a_y = \ddot{y} = \frac{v^2}{R} \tag{17}$$

$$\begin{aligned} dv &= v_i - v_{i-1} \\ dt &= \frac{dx}{v_i} \\ a_x = \ddot{x} &= \frac{dv}{dt} \end{aligned} \tag{18}$$
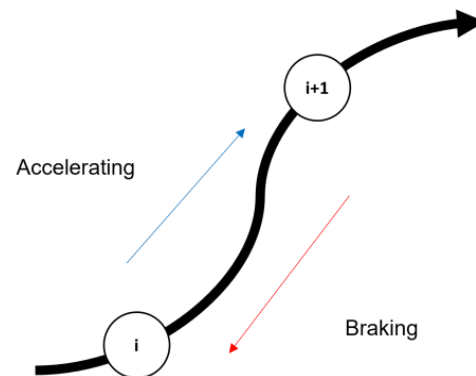

Figure 12. Illustration of quasi-steady-state simulation.

From these calculations, the intersection of the two velocities, and acceleration and deceleration side velocities with respect to distance, are used as the braking start point, and the limit performance of the vehicle in the quasi-steady state can be predicted.

The computation run time is very fast; a single-lap simulation requires less than 30 s; this makes it possible to analyze the sensitivity of lap times when various parameters are changed.

4. Final Gear Ratio and Electric Motor Gear Ratio Study

4.1. Simulation Calculation Conditions

To evaluate the vehicle performance of the proposed small-race car, the power supply voltage of the electric motor was 77 V, as shown in Table 2. A reduction gearbox was added to the electric motor, the ICE and electric motor speeds were individualized, a program was created to allow the torque and speed of the electric motor to be varied, and the reduction ratio of the electric motor and final gear ratio were changed for lap-time simulations.

The primary reduction ratio of the ICE was set to 3.12, and no lower than 3500 rpm was used in this study because the ICE halts at low speeds when starting the vehicle. Therefore, the initial speed at start-up was set to 3500 rpm in the first gear. The ICE speed is increased when the ICE speed reaches 10,000 rpm, and the value at the 6th gear and 10,000 rpm is held constant in the simulation after the 6th gear and 10,000 rpm. The ICE and electric motor shaft torques were modeled by polynomial approximation using the two-dimensional data in Figures 6 and 8. The simplified vehicle model in Table 3 was used for other basic parameters. The evaluation circuit was an 800 m closed circuit with a series of left and right turns, as shown in Figure 13.
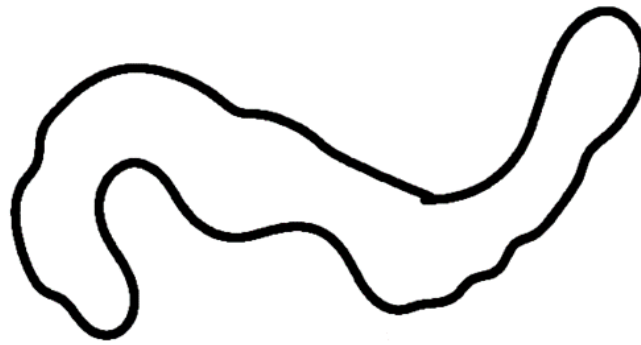
Figure 13. Schematic of evaluation 800-m circuit.

Table 3. Vehicle data.

General Data		Engine Data	
Mass [kg]	369.7	Thermal Efficiency [%]	35
Driven Type	2WD	**Transmission**	
Aerodynamics Data		Gear 1	2.642
Drag Coefficient	0.8	Gear 2	1.812
Frint Area [m^2]	1.2	Gear 3	1.318
Air Density [kg/m^3]	1.1	Gear 4	1.04
Tire Data		Gear 5	0.888
Tire Radius	0.128	Gear 6	0.785
Rolling Resistance	0.03	Final Drive Ratio	3.145
Longitudinal Friction	1.4	Drive Efficiency	3.145
Lateral Friction	1.5		

4.2. Analysis Result and Discussion

Simulations were performed on a small hybrid race car with varying final and electric motor reduction gear ratios. The objective was to minimize the lap times, and the role of the powertrain was to achieve the maximum possible acceleration in each velocity range. There is a trade-off between lowering the final gear ratio, which reduces the acceleration that can be generated because of the reduction in axle torque, and raising it too high, which reduces the maximum speed owing to power unit speed limitations, and causes tires to reach their slip limits, resulting in excess powertrain dynamic performance.

Figure 14 shows analysis results with final gear ratios of 1, 12, and 30; this figure shows that, when the final gear ratio is 1, the overall slope of speed is low, and when the final gear ratio is 30, the speed hits its limit. In addition, the speed slope is always the same when comparing final gear ratios 12 and 30, indicating that a higher gear ratio exceeds the limit of the tire's longitudinal force, resulting in a waste of the powertrain's dynamic performance.
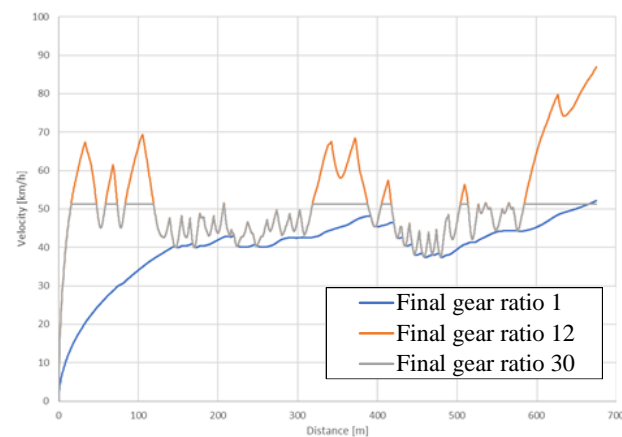
Figure 14. Relationship between distance and vehicle velocity for each final gear ratio.

The reduction ratio of the electric motor has a small setting range of 2, 5, and 15 for the gear ratio because the electric motor generates more torque at lower speeds owing to its characteristics. The relationship between distance and velocity for each reduction ratio of the electric motor is shown in Figure 15. The speed range where the characteristics of the electric motor can be utilized is the high-velocity range, and the difference between each gear ratio appears at the point where the highest velocity is reached in one lap. Extremely large electric motor gear ratios exceeded the tire's limits of longitudinal force, and nullify the advantages of the hybrid system.
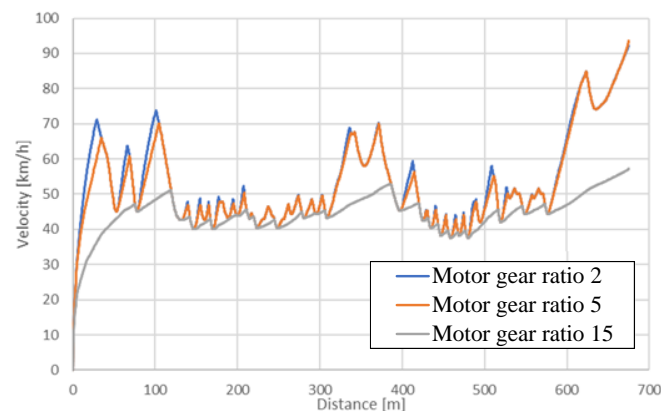

Figure 15. Relationship between distance and vehicle velocity for each electric motor gear ratio.

The relationship between the final gear ratio and obtained lap time is shown in Figure 16, and the relationship between the electric motor reduction gear ratio and running time is shown in Figure 17. The simulations on this evaluation circuit produced the fastest results when the final gear ratio was 12 and the electric motor reduction gear ratio was 2.
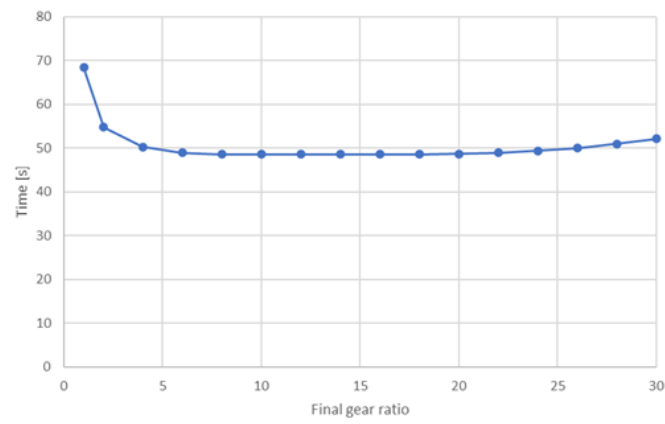
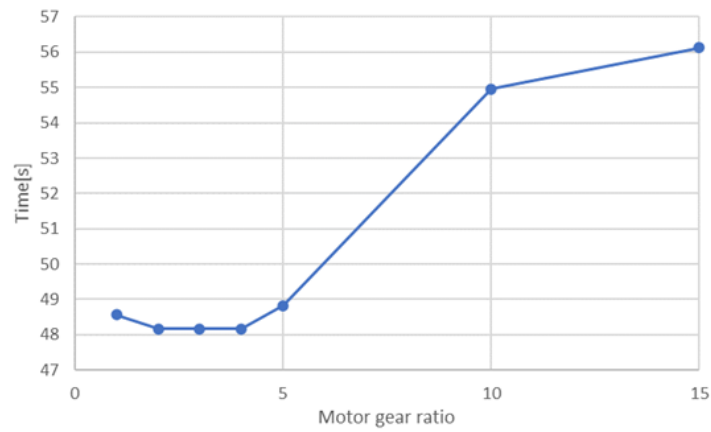**Figure 16.** Relationship between final gear ratio and lap time.

Figure 17. Relationship between electric motor gear ratio and lap time.

The analysis results presented in this study can be used to construct control algorithms for the proposed hybrid system.

5. Conclusions

As a fundamental study for acquiring a computational algorithm for a multi-input, multi-output servo model in a hybrid system proposed for a small race car, this study analyzed the electric motor reduction ratio and final reduction ratio for vehicle performance optimization through simulation. The simulation results showed that the optimal settings were obtained by changing the final reduction ratio and the electric motor reduction ratio on an 800 m evaluation circuit.

In this study, the effectiveness of the hybrid system with the proposed mechanism as a competition vehicle is compared with conventional planetary gear mechanisms and in-wheel electric vehicles, and a brief introduction of the modeling method is given. In addition, the theory and utility of quasi-steady-state lap-time simulation, which models the vehicle and predicts its performance in a simplified manner, is presented as a powerful tool for optimizing powertrain systems. More practical simulations can be expected by extending the model, and parameter-sensitivity analysis can be performed outside the scope of this research.

In the future, based on the analysis results, we will proceed with the development and design of an actual vehicle, and simulation of closed-loop circuit driving. We will also develop a vehicle-dynamics simulation tool that includes more detailed non-linear elements for building control algorithms and predicting complex vehicle motion phenomena that occur when the vehicle is driven. Especially, we will consider a differential mechanism. When considering the cornering of race cars, the vehicle has a yaw angular velocity and track, which causes a difference in ground speed between the left and right wheels; this effect also causes a difference in the slip ratio of the tire contact patch, so a differential mechanism that allows for differences in wheel speed is necessary for vehicle cornering. In future studies, we would like to examine the differential mechanism required for race cars, and the control of the locking mechanism according to the situation.

Author Contributions: Conceptualization, H.K. and T.N.; methodology, I.K.; software, I.K.; validation, K.O., D.U. and T.N.; formal analysis, K.O.; investigation, D.U.; writing—original draft preparation, I.K.; writing—review and editing, K.I., M.H.B.P., T.K. and A.E.; visualization, I.K.; supervision, H.K.; project administration, T.N. All authors have read and agreed to the published version of the manuscript.

Institutional Review Board Statement: Not applicable.

Informed Consent Statement: Not applicable.

Conflicts of Interest: The authors declare no conflict of interest.

References

1. Perez, L.; Pilotta, E. Optimal power split in a hybrid electric vehicle using direct transcription of an optimal control problem. *Math. Comput. Simul. Tegucigalpa* **2004**, *79*, 1959–1970. [CrossRef]
2. Viehmann, A.; Rinderknecht, S. Investigation of the Driving Comfort of the DE-REX Powertrain based on Vehicle Measurements. *Int. Fed. Autom. Control. Pap. Online* **2019**, *52*, 103–108. [CrossRef]
3. Travis, E.; Torrey, J.; John, E.; Denise, M.; Jada, B. Tracked vehicle physics-based energy modelling and series hybrid system optimisation for the Bradley fighting vehicle. *Int. J. Electr. Hybrid Veh.* **2020**, *12*, 1–14.
4. Jing, L.; Xin-ran, W.; Lin-hui, L.; Ya-fu, Z.; Shu-zhou, Y.; Xiu-jie, L. Plug-in HEV energy management strategy based on SOC trajectory. *Int. J. Veh. Des.* **2021**, *82*, 1–17.
5. Zainab, A.; El, A.; Daniela, C.; Luis, M. Energetic macroscopic representation and inversion based control of fuel cell in a series hybrid race vehicle system. *Int. J. Electr. Hybrid Veh.* **2022**, *12*, 197–213.
6. Wu, G.; Zhang, X.; Dong, Z. Powertrain architectures of electrified vehicles: Review, classification and comparison. *J. Frankl. Inst.* **2015**, *352*, 425–448. [CrossRef]
7. Mohammadpour, M.; Rahnejat, H. Dynamics and efficiency of planetary gear sets for hybrid powertrains, Proceedings of the Institution of Mechanical Engineers. *Part C: J. Mech. Eng. Sci.* **2015**, *230*, 1359–1368.

8. Sato, Y.; Narita, T.; Kato, H.; Okamoto, T. Proposal of Power Synthesis Mechanism in Hybrid System for Compact Racing Car: A Fundamental Consideration on Structural Design and Vehicle Movement Performance. *Proc. Sch. Eng. Tokai Univ. Ser. E* **2018**, *43*, 31–37.
9. Lot, R.; Evangelou, S. Lap Time Optimization of a Sports Hybrid Electric. *Veh. Proc. World Congr. Eng.* **2013**, *3*, 1711–1716.
10. Lambert, S.; Maggs, S.; Faithfull, P.; Vinsome, A. Development of A Hybrid Electric Racing Car. In *IET HEVC 2008-Hybrid and Eco-Friendly Vehicle Conference*; IET: London, UK, 2008. [CrossRef]
11. Edward, D. The Robust Control of a Servomechanism Problem for Linear Time Invariant Multivariable Systems. *IEEE Trans. Autom. Control* **1976**, *21*, 25–34.
12. Wolter, W. *Linear Multivariable Control–A Geometric Approach*; Springer: Berlin/Heidelberg, Germany, 1978; pp. 203–210.
13. Milliken, W.; Milliken, D. *Race Car Vehicle Dynamics*; Society of Automotive Engineers, Inc.: Warrendale, PA, USA, 1995; p. 343.
14. Casanova, D.; Sharp, R.; Symons, P. Minimum Time Manoeuvring: The Significance of Yaw Inertia. *Veh. Syst. Dyn.* **2000**, *34*, 77–115. [CrossRef]
15. Bianco, N.; Lot, R.; Gadola, M. Minimum time optimal control simulation of a GP2 race car. *Proc. Inst. Mech. Eng. Part D J. Automob. Eng.* **2017**, *232*, 1180–1195. [CrossRef]
16. Patton, C. Development of Vehicle Dynamics Tools for Motorsports. Doctor of Philosophy Dissertation, Oregon State University, Corvallis, OR, USA, 2013.
17. Brayshaw, D.; Harrison, M. A quasi steady state approach to race car lap simulation in order to understand the effects of racing line and centre of gravity location. *Proc. Inst. Mech. Eng. Part D J. Automob. Eng.* **2005**, *219*, 725–739. [CrossRef]
18. Siegler, B.; Deakin, A.; Crolla, D. Lap Time Simulation: Comparison of Steady State, Quasi- Static and Transient Racing Cornering Strategies. *SAE Technical Paper* **2000**. [CrossRef]
19. Pacejka, H. *Tire and Vehicle Dynamics Third Edition*; Elsevier Ltd.: Oxford, UK, 2012; pp. 176–183.
20. Koutrik, S. Optimal Control for Race Car Minimum Time Maneuvering. Master of Science Thesis, Delft University of Technology, Delft, The Netherlands, 2015.